Radio Frequency Plasma Generator Impedance Matching System

Miles Houston, Owen Liao, Miles McLean, Wilson Wu, Jacky Zhao

***Abstract*—** Plasma etching is a critical process in semiconductor manufacturing that relies on the precise delivery of Radio-Frequency (RF) power to varying gas loads. This paper presents the design of a dual-frequency RF plasma generator and impedance matching system capable of driving Oxygen and Argon plasmas at 13.6 MHz and 2.45 GHz. To address the significant impedance mismatch between standard 50Ω sources and the complex plasma chamber load ($Z_{chamber}$ = 14.85 - j64.28), we implemented and analyzed two distinct matching networks: a distributed double-stub tuner and a lumped-element (LC) L-network. Utilizing a cost-effective dual-generator approach—pairing a Diener Electronics 100W unit with a Mini-Circuits 50W solid-state source—we successfully circumvented the high costs associated with broadband amplifiers. The double-stub matching network was designed using Smith Charts. The LC matching network was derived and validated using LTSpice analysis. Simulation results confirmed that the LC network successfully transformed the complex load to a resistive 50Ω input with negligible phase shift, ensuring efficient power transfer of 20W to the Oxygen plasma and 5W to the Argon plasma. This work demonstrates a viable, high-efficiency solution for multi-mode plasma etching systems.

I. INTRODUCTION

Plasma is a high-energy phase of matter characterized by a significant portion of free, charged particles. The use of plasma in scientific and industrial processes like material science, fusion energy, and semiconductor manufacturing has been found to be particularly useful[1]. Within the field of semiconductor manufacturing, plasma is used to precisely remove material from Silicon on Insulator (SOI) wafers to realize complex integrated circuits, in a process called plasma etching. The most straightforward method of generating plasma consists of coupling a RF power generator to a plasma chamber where power is delivered to a chamber, exciting the gas to its plasma state. However, modern etching needs desire multiple operating modes, whereby plasma generators should be able to support different gasses (e.g. Oxygen and Argon) at multiple power and frequency configurations (e.g. 1-20 watts and 13.6MHz - 2.45GHz). These diverse operating settings make it difficult to deliver sufficient power to the plasma chamber due to a poor impedance match between the generator and plasma chamber[2]. For this purpose, a matching network needs to be used to maximize power delivery to the chamber. In this configuration, the RF plasma generator consists of 4 parts: a RF generator, a feedline that delivers power to the chamber, a matching network placed either in parallel with the load or on the feedline, and a plasma chamber. In our work, we implement an RF Plasma Generator for Oxygen and Argon at operating frequencies 13.6MHz and 2.45GHz. We design separate LC and double stub matching networks to ensure 20 and 5 watts are delivered to the Oxygen and Argon, respectively. Due to the cost and availability of high-bandwidth and high-power RF generators, our design employs two generators for the two different operational frequencies.

II. SYSTEM MODEL

The RF Plasma Generator is comprised of 4 parts. (1), the RF-Generator, we use a setup comprised of two generators for the different operating frequencies. (2) A feedline of a standard 50Ω. (3) Two separate matching networks described below). (4) A Plasma chamber measured to have impedance$Z_{chamber} = 14.85 - j64.28$.

The LC matching network for the plasma system contains 2 components to balance the load. We use a lowpass L-shaped matching network with a shunt capacitor then a series inductor for maximum power transfer as pictured below[3]:

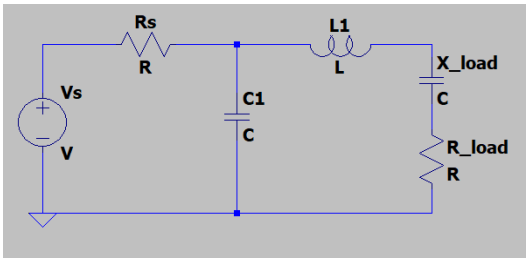

Figure 1. LC Matching Network Circuit to Evaluate for.

For LC matching, the inductor in series directly modifies the reactance value, but a capacitor in shunt directly modifies the susceptance value, resulting in a non-linear effect on impedance from the shunt[3]. This means that the series inductor can modify the imaginary part of the impedance, while the shunt capacitor can modify both the real and imaginary parts of the impedance. With these two variable components, we have two degrees of freedom that allows us to match the real and imaginary parts of the input impedance to the source impedance for maximum power transfer.

Solving the complex impedance of the Z_{in} (LC matching network and load) in the derivation enables us to obtain the values of capacitance and inductance through the maximum power transfer theorem. The theorem states that for the

maximum power to reach the load, $Z_{load} = Z_s$. From Z_s being purely real, we get $R_{in} = R_s$ and $X_{in} = 0$, such that we can solve for L and C:

$$R_s = \frac{R_{load}^2 + (X_{load} + X_L)^2}{R_{load}} \quad (1)$$

$$wC = \frac{X_{load} + X_L}{R_{load}^2 + (X_{load} + X_L)^2} \quad (2)$$

However, equations 1 and 2 assume that the real part of the complex load impedance is less than the real part of the source impedance. That is, $R_s > R_{load}$. If this is not the case, then a different configuration of the LC matching network must be used[6]. Because the source impedance of the chosen generator is greater than the load impedance for all the cases described in this project, equations 1 and 2 were used[7]. The different configuration for when the load impedance is greater than the source impedance is discussed in the Appendix section[8].

For the double stub matching network, we use shorted stubs where y_a, y_b give the normalized admittance values for the stub furthest and closest to the load, respectively. $y_L$is given as the normalized load admittance:

$$y_L = \frac{Y_L}{Y_0} = g_L + ib_L \quad (3)$$

$$y_a = \frac{y_b + j\tan(\beta l)}{1 + jy_b\tan(\beta l)} - j\cot(\beta d_1) \quad (4)$$

$$y_b = g_L + j(b_L - \cot(\beta d_2)) \quad (5)$$

where β is the phase constant in the feedline. We use Smith Charts (see appendix) to find the matching condition $y_a = 1$to solve for stub lengths [4].

III. Results

A. Stub Matching

We perform a double short-circuited stub matching procedure both graphically using a Smith chart and numerically using Python. The two methods yielded the same stub lengths. Stub 1 is parallel to the load and stub 2 is at a fixed distance away of $l = 0.125\lambda$. Different stub lengths are required for the Oxygen and Argon plasmas, whose load impedances are written in Table 2.

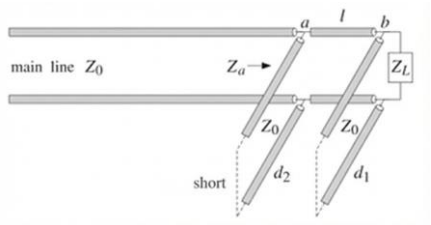

Figure 2. This image shows the double stub matching network.

For the Oxygen plasma, we calculate normalized load admittance $y_L = 0.30 + j0.75$. The lengths of the two stubs are found graphically and are $(d_1, d_2) = (0.180, 0.100)$ measured in units of wavelength.

We perform the same procedure for the Argon plasma matching. Again, the load admittance is $y_L = 0.40 + j0.95$, and the lengths of the stubs are $(d_1, d_2) = (0.147, 0.125)$.

Stub lengths are summarized in Table 1 for each case Details on our usage of the Smith chart, and our procedure can be found in the appendix [4].

	Case A	Case B	Case C	Case D
Gas and Frequency	Argon, 13.6 MHz	Argon, 2.45 GHz	Oxygen, 13.6 MHz	Oxygen, 2.45 GHz
$d1$	$3.24m$	$0.018m$	$3.97m$	$0.022m$
$d2$	$2.76m$	$0.125m$	$2.2m$	$0.012m$

Table 1. This table contains the stub lengths for each case.

B. LC Matching

Using equations 1 and 2, we solve for L and C with given R_s, Z_{load}, and frequency for the 2 frequencies and gases for 4 total cases.

	Case A	Case B	Case C	Case D
Gas and Frequency	Argon, 13.6 MHZ	Argon, 2.45 GHz	Oxygen, 13.6 MHz	Oxygen, 2.45 GHz
Impedance of gas (Taken at average of 4W)	500 - j150	500 - j150	300- j750	300- j750
Power Needed	3 to 5W	3 to 5W	18 to 20 W	18 to 20 W
Impedance of Chamber (We chose the experimental 13.6 MHz impedance)	14.85- j64.28	14.85- j64.28	14.85- j64.28	14.85- j64.28
Total Impedance	18.87- j44.64 [Ω]	18.87- j44.64 [Ω]	26.10- j56.99 [Ω]	26.10- j56.99 [Ω]
Capacitance	3 x 10^{-10} F	1.669 x 10^{-12} F	2.24 x 10^{-10} F	1.243 x 10^{-12} F
Inductance	8.06 x 10^{-7} H	4.474 x 10^{-9} H	9.592 x 10^{-7} H	5.325 x 10^{-9} H

Table 2. This table contains the values for the different cases that the matching networks were designed for. It also contains the capacitance and inductance values for the LC circuit matching network.

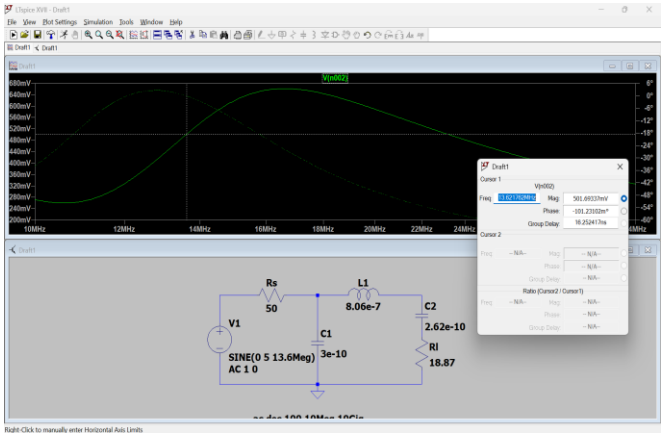

Figure 3. This image shows the LTSpice AC Analysis simulation of Case A in Table 1.

In Figure 3, the voltage of the node after the 50 Ohm resistor was measured. This was because the 50 Ohm resistor represents the source impedance. Thus, the actual voltage being generated by the generator would be measured after the source impedance resistor. The importance behind this measurement was to observe the phase of the voltage signal. Ideally, based on our calculations, the voltage signal should not have any phase shift. However, as seen in Figure 3, the phase was around –101.2 millidegrees. This error from 0 degrees can be attributed to the rounding of the inductance and capacitance values shown in the circuit to cancel out the imaginary component of the load impedance. Thus, this error can be considered negligible.

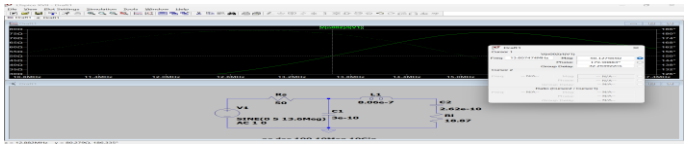

Figure 4. This image shows the measured input impedance at 13.6 MHz of the circuit shown in Figure 2 for Case A.

The next step in confirming the efficacy of the LC matching network was to measure the input impedance. In Figure 4, it shows that the input impedance at 13.6MHz was approximately 50 Ohms, which matches the source impedance. Thus, the source impedance sees 50 Ohms, enabling for maximum power to be delivered to the load.

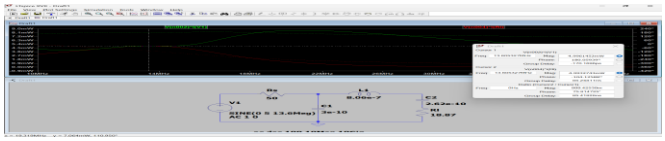

Figure 5. This image shows the power transfer measurements from the source to the load for the circuit shown in Figure 2 for Case A.

Based on the results presented in Figure 5, it can be concluded that the maximum power was delivered from the source to the load. This is shown with the power generated from the source measured at about 5 mV, which was the same as the power measured at the load impedance, meaning that all the power generated from the source was transferred to the load. Therefore, the LC matching network successfully configured the input impedance to 50 Ohms, which enabled maximum power transfer from the source generator to the load.

Performing the same steps shown above in Figure 3 to Figure 5, the values for the LC matching networks for the different cases shown in Table 2 were tested to see if maximum power was transferred from the source generator to the load.

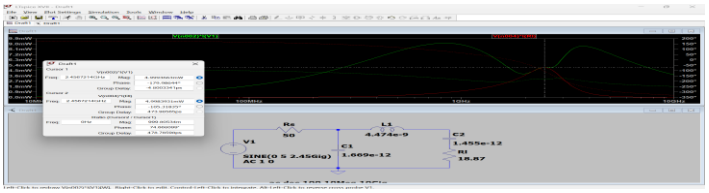

Figure 6. This image shows the power transfer measurement for the inductance and capacitance values for Case B. The maximum power transfer was achieved as 5 mV was transferred from the source to the load.

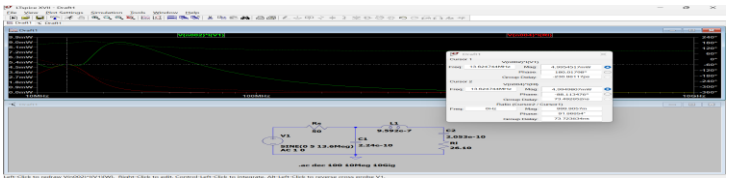

Figure 7. This image shows the power transfer measurement for the inductance and capacitance values for Case C. The maximum power transfer was achieved as 5 mV was transferred from the source to the load.

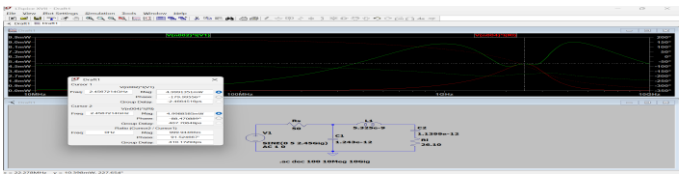

Figure 8. This image shows the power transfer measurement for the inductance and capacitance values for Case D. The maximum power transfer was achieved as 5 mV was transferred from the source to the load.

Although it is shown in the testing circuits in LTSpice that the maximum power transfer was only 5 mV, the amplitude of the AC signal is based on the generator chosen, which was 1 V in this case. Thus, 5 mV is not the actual power transferred when the plasma generator is built, as the power generated by the source depends on the maximum voltage amplitude of the specific chosen generator, instead we can read this result as the power transferred is 5% of the maximum voltage amplitude. The testing shown in Figure 3 to Figure 8 simply shows that no matter what power is generated from the source, the maximum power will be delivered as long as the input impedance derived from the LC matching network matches the source impedance. Furthermore, in the circuits shown in LTSpice, there is a capacitor in series with the load resistor.

This is because complex impedance values must be simulated through the addition of capacitors or inductors in the software as it has no built-in method of just adding an imaginary part to the resistor. Thus, the capacitor and resistor in series represent the total complex load impedance of the gas chamber and gas shown in Table 2. Due to the total complex load impedance having a negative imaginary part, a capacitor was used to simulate this imaginary component. The value of said capacitor was calculated using the equation

$$C = \frac{1}{\omega X_{load}} \text{ where } \omega = 2\pi f \qquad (6)$$

If the frequency or total complex load impedance were to change, then the inductance and capacitance values can be modified using equations 1 and 2. Finally, if the imaginary component of the total complex load impedance is positive, then an inductor should be used to represent that in the simulation. The value of this inductor can be found using the equation

$$L = \frac{X_{load}}{\omega} \text{ where } \omega = 2\pi f \qquad (7)$$

IV. Discussion

For our RF signal generator, we choose to use two different signal generators to avoid the very high bandwidth and high-power delivery requirements, necessitated by a shared generator. For the 13.6 MHz operating mode, we choose a 100-watt generator produced by Diener Electronics. The model has a characteristic impedance of a standard 50Ω and can be bought for ~$5000 USD with a quote. We pair this generator with a RFS-2G42G5050X High Power Signal Source, available for $695. This model has an output capacity of 50 watts and a characteristic impedance of 50Ω. We choose two generators of the same impedance for consistency across our matching networks. Both generators provide more wattage than what is required by the oxygen plasma, and our matching networks provide sufficient impedance match that we are able to meet the 5- and 20-watt power delivery specifications.

For the LC matching network, based on results seen in Figure 2 to Figure 7, the system that was designed enables maximum power transfer from the source generator to the load. Due to the low capacitance and inductance values shown in Table 1 and the results they produce, it can be reasonable to implement a transmission line with said values between the source generator and the load. This is because the feed line is assumed to be purely resistive while actual transmission lines have both resistive, capacitive, inductive, and conductive properties. Thus, using the system designed and equations used to calculate the different inductive and capacitive values, engineers can order or manufacture transmission lines with those properties. Furthermore, the circuit shown in Figure 1 is the most ideal configuration for an LC matching network when the real part of the source impedance is greater than the real part of the load impedance as it only uses 1 capacitor and 1 inductor. It is true that the image shows 1 resistor in series with the source and 1 extra capacitor in series with the load. However, these were only inserted for simulation purposes. If the circuit were to be implemented in the real world, the resistor in series with the source would be a property of the source and feed line while the capacitor in series with the load would also be a property of the load. Thus, for the real-world equivalent circuit, there would only be 1 inductor and 1 capacitor. During the design of this circuit, the math could have been simplified if another capacitor or inductor was inserted in series with the total complex load impedance to cancel out the imaginary part. Then, the circuit could be analyzed assuming that the load is completely real. Even though the math would have been simplified, this would not have been beneficial for manufacturers or the customer as that extra capacitor could add millions of dollars in cost when a large quantity of the product is produced. Therefore, the most cost-effective design would only consist of 1 inductor and 1 capacitor.

V. Conclusion

The design of our two matching networks yielded the desired performance of 5- and 20-watt power delivery to the Argon and Oxygen gas, respectively. We complete this at two operational frequencies, 13.6 MHz and 2.45 GHz while maintaining a compact and cost-effective solution. Thus, the generator satisfies the projects' design goals. We note, as possible for future extensions, one could reduce the cost of the signal generators by exploring combinations of signal generators and amplifiers. In our solution, searching for a “one size fits all" increased the complexity and cost of the signal generators. Additionally, for better matching performance, a dual RLC and double stub matching network could be used.

APPENDIX

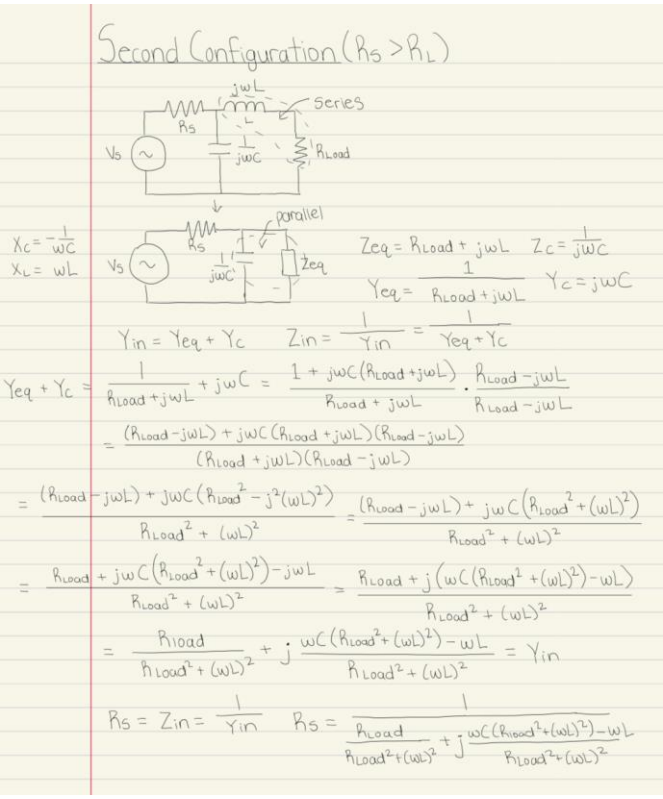

Figure 9 This image shows the first section of calculations for solving the circuit for inductance and capacitance with a real valued load.

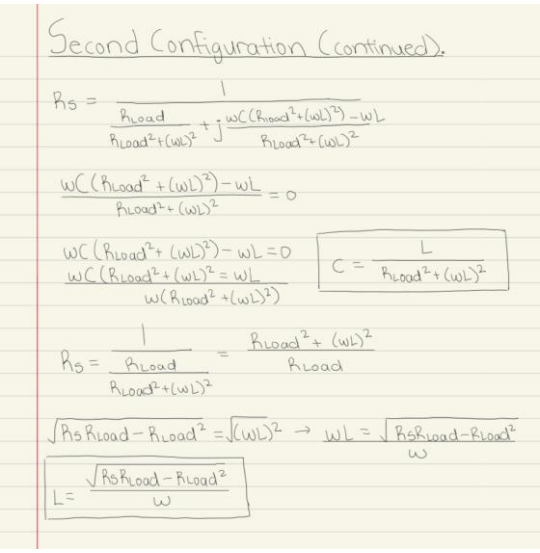

Figure 10. This image shows the second section of calculations for solving the circuit for inductance and capacitance with the final equations to calculate with a real valued load.

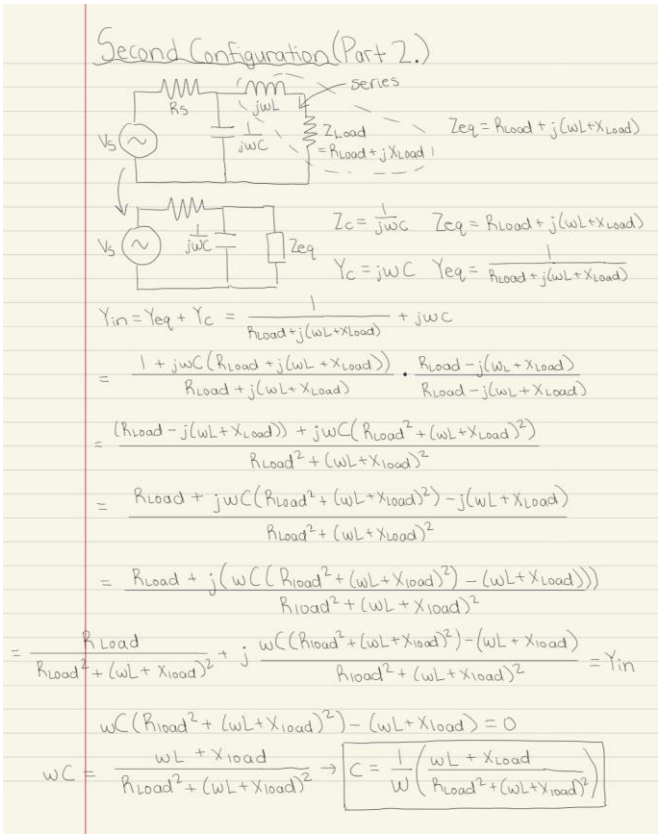

Figure 11. This image shows the third section of calculations for solving the circuit for inductance and capacitance with a complex load.

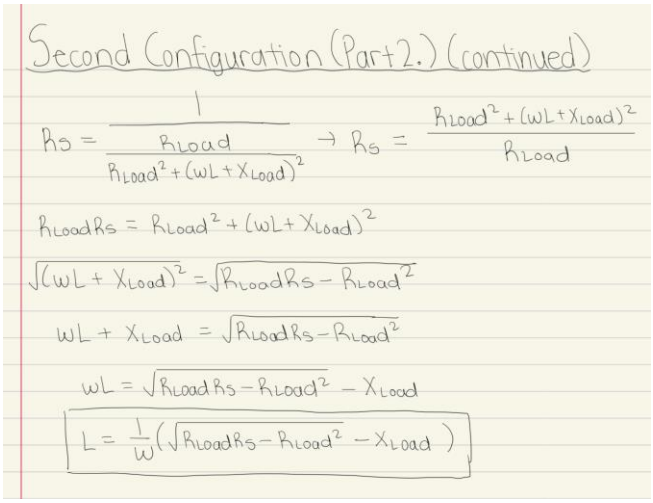

Figure 12. This image shows the final section of calculations for solving the circuit for inductance and capacitance with a complex load.

The images below show the calculations for the LC matching network if the real part of the load impedance is greater than the real part of source impedance. Although this configuration was not used in this project due to its incompatibility with the design specifications and values, it is important to show due as

changes to either the load impedance or source impedance could affect the configuration of the designed circuit.

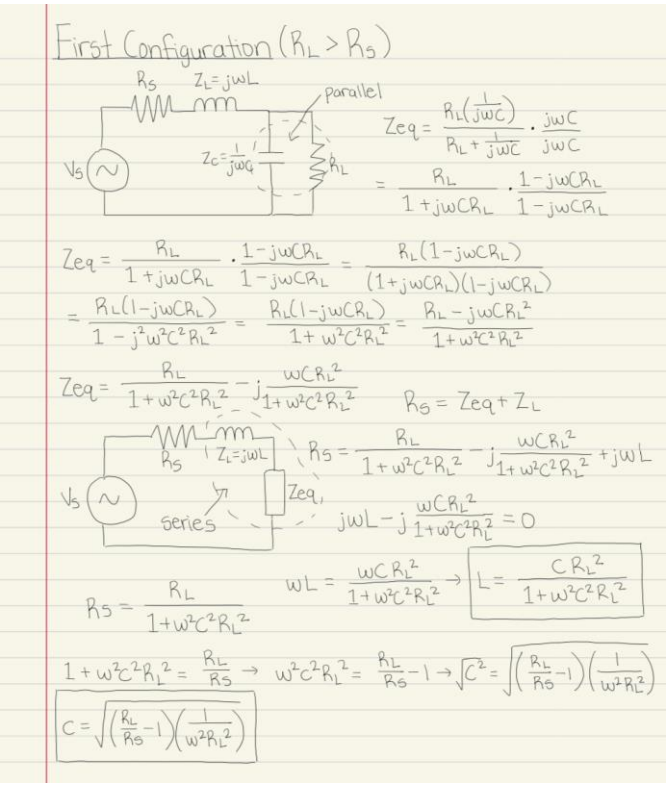

Figure 13. This image shows the calculations for the configuration of the LC matching network if the real part of the load impedance is greater than the real part of the source impedance. These calculations assume that the load is purely real.

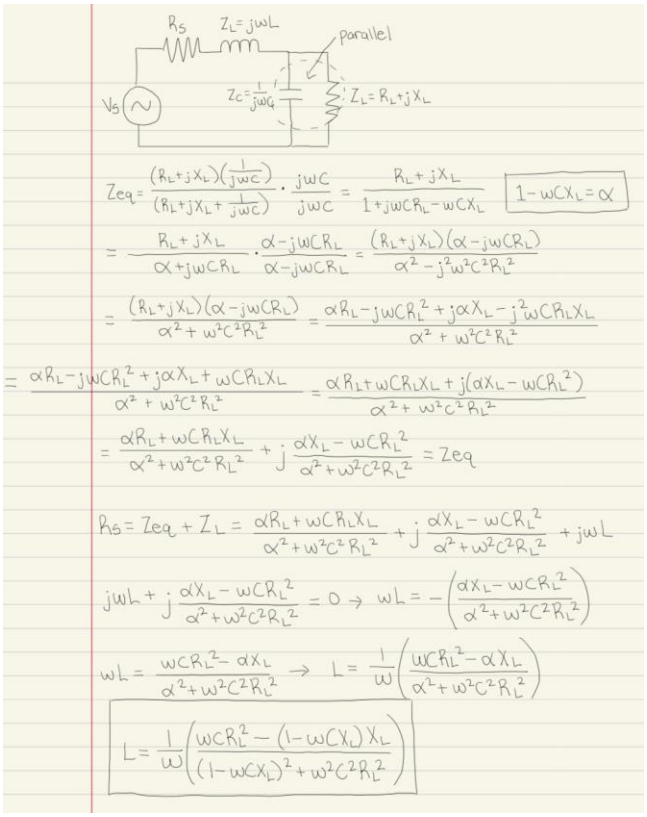

Figure 14. This figure shows the first section of calculations for when the configuration shown in Figure 12 has an imaginary component in the load impedance.

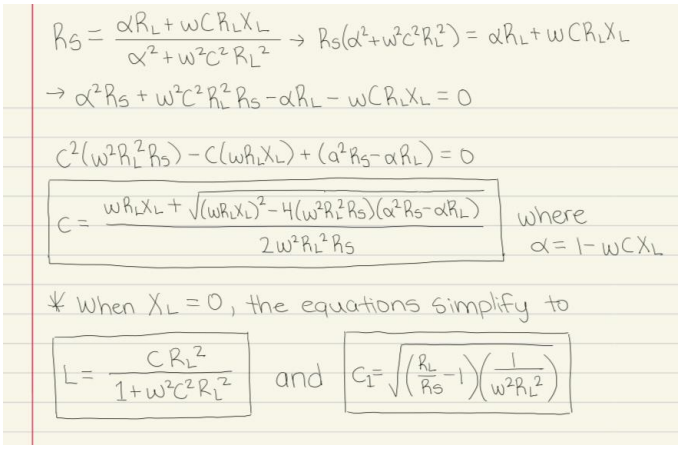

Figure 15. This figure shows the final section of the calculations for when the configuration shown in Figure 12 has an imaginary component in the load impedance. When the load impedance is 0, the equations simplify to the ones shown in Figure 12.

```python
def gamma_in(zL, l, d1, d2):
    """
    Returns reflectance at input. l, d1, d2 are in units of wavelength. zL
    is the normalized load impedance.
    """
    beta = 2 * np.pi
    yL = 1.0 / zL

    yb = yL + 1j * np.tan(beta * d2)
    ya_line = (yb + 1j * np.tan(beta * l)) / (1 + 1j * yb * np.tan(beta * l))
    ya = ya_line + 1j * np.tan(beta * d1)


    zin = 1 / ya
    gamma = (zin - 1) / (zin + 1)
    return abs(gamma)
```

Figure 16. Function definition for calculating the reflectance coefficient at the load for a given load impedance and double stub lengths[10].

The images below (Figures 17-19) show the graphical methods used to find stub lengths for Oxygen and Argon.

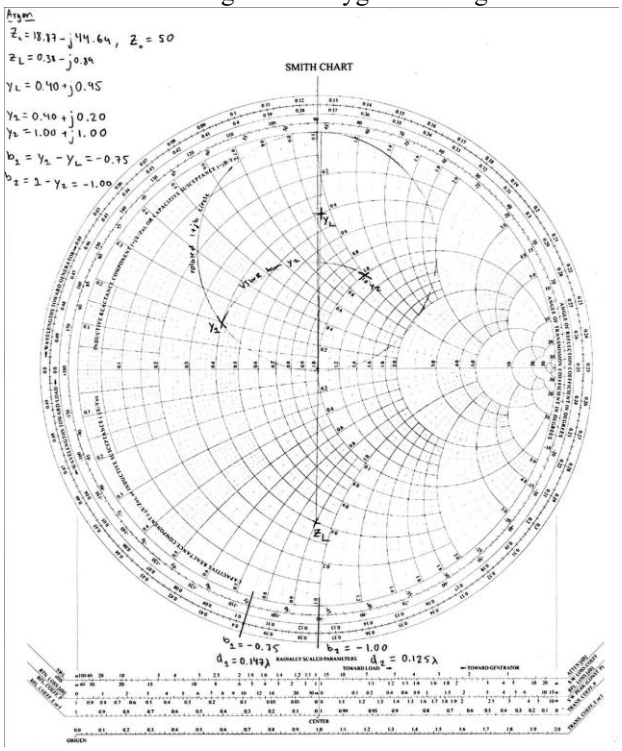

Figure 17. Smith chart shorted double-stub solution for Argon. The solution with shorter stubs was selected.

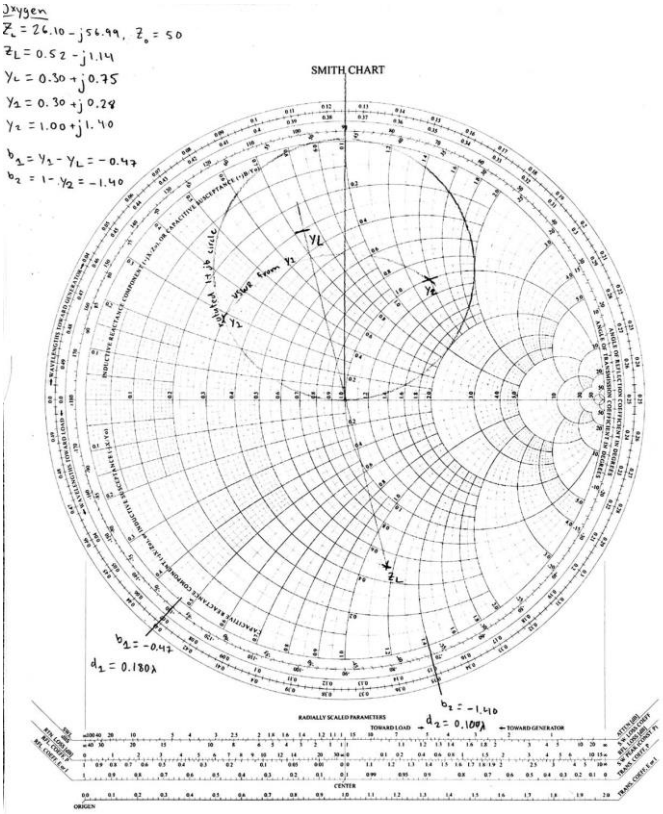

Figure 18. Smith chart shorted double-stub solution for Oxygen. The solution with shorter stubs was selected.

```
Argon
  solution 1: d1 = 0.362, d2 = 0.449, |Γ| = 4.58e-16
  solution 2: d1 = 0.147, d2 = 0.125, |Γ| = 2.48e-16

Oxygen
  solution 1: d1 = 0.377, d2 = 0.452, |Γ| = 5.98e-16
  solution 2: d1 = 0.180, d2 = 0.108, |Γ| = 1.57e-16
```

Figure 19. Python output of stub lengths $d1, d2$ and reflection coefficient |Γ| for Oxygen and Argon[10].

References and Footnotes

A. References

[1] National Research Council, Plasma Processing of Materials: Scientific Opportunities and Technological Challenges. Washington, DC: The National Academies Press, 1991.

[2] S. Sarkar, “Understanding the Need of Matching Networks - Rahsoft,” *Rahsoft*, Apr. 13, 2021. https://rahsoft.com/2021/04/13/understanding-the-need-of-matching-networks/ (accessed Dec. 10, 2025).

[3] S. Sarkar, “Understanding the Concept of RLC Matching Circuits - Rahsoft,” *Rahsoft*, Aug. 16, 2021. https://rahsoft.com/2021/08/16/understanding-the-concept-of-rlc-matching-circuits/

[4] “Electromagnetic Waves and Antennas.” Available: https://gctjaipur.wordpress.com/wp-content/uploads/2015/08/electromagnetic-waves-and-antennas.pdf

[5] “Double-Stub Matching.” Accessed: Dec. 10, 2025. [Online]. Available: https://web.eecs.utk.edu/~ggu1/files/ECE341Notes_10_DoubleStubMatching.pdf
[6] S. Sadeghi, “The L-shaped Matching Network,” Impedans, Mar. 29, 2023. https://www.impedans.com/the-l-shaped-matching-network/
[7] EEStream, “Lecture 4 - Impedance Matching Networks,” *YouTube*, Apr. 21, 2020. https://www.youtube.com/watch?v=TyGYbmo969A (accessed Dec. 10, 2025).
[8] Matthew Spencer, “HMC E157 Lec08 V01 L Matching Networks Introduction,” YouTube, Sep. 30, 2024. https://www.youtube.com/watch?v=vmLxJWMwZos (accessed Dec. 10, 2025).
[9] S. J. Orfanidis, “S-Parameters,” in *Electromagnetic Waves and Antennas*, Rutgers University, 2016, ch. 12. Available: https://daskalakispiros.com/files/Ebooks/Electromagnetic%20Waves%20and%20Antennas%20S%20Orfanidis/ch12.pdf (accessed Dec. 10, 2025).
[10] Miles Houston, “EE 18 Final Project Double Stub,” 2025. Python. Available: https://github.com/owenwliao/ee-18-final-project-stub-matching/tree/main